

## Macrophage Targeting of Azidothymidine: A Promising Strategy for AIDS Therapy\*

RAIMAR LÖBENBERG and JÖRG KREUTER

### ABSTRACT

Macrophages play an important role in the immunopathogenesis of AIDS. The objective of this study was to investigate the possibility of specific targeting of antivirals such as azidothymidine (AZT) to macrophages, using nanoparticles as a colloidal drug carrier. The body distribution of AZT bound to nanoparticles and as a control solution was studied in rats after intravenous and peroral administration. <sup>14</sup>C-Labeled AZT was bound to nanoparticles in the presence of bis(2-ethylhexyl)sulfosuccinate sodium. The radioactivity was measured in different organs including those containing large numbers of macrophages. After intravenous injection, the concentrations of AZT were up to 18 times higher in organs belonging to the reticuloendothelial system (RES) when the drug was bound to nanoparticles than after injection of an aqueous AZT solution. Likewise, after oral administration the nanoparticle formulation delivered AZT more efficiently to the RES than the aqueous solution. In addition, the blood concentration was significantly higher after oral administration of nanoparticles. These results demonstrate that nanoparticles are a promising drug-targeting system for AZT to the RES organs. The increase in drug availability at the sites containing abundant macrophages may allow a reduction in dosage to avoid systemic toxicity.

### INTRODUCTION

CELLS OF THE RETICULOENDOTHELIAL SYSTEM (RES), especially monocytes/macrophages (MO/MAC) and possibly also endothelial cells, play an important role in HIV infection and the immunopathogenesis of AIDS.<sup>1-3</sup> These cells serve as a reservoir for the virus and are believed to be responsible for its dissemination throughout the body and especially into the brain.<sup>4,5</sup> The ability to access RES cells is therefore critical to the success of AIDS therapy.

Colloidal drug carriers such as nanoparticles have been shown to accumulate in the RES. Nanoparticles are solid, biocompatible polymeric particles, ranging in size between 10 and 1000 nm, in which drugs can be incorporated.<sup>6</sup> In addition to their ability to accumulate in the RES, it has been shown that by manipulation of their surface properties, nanoparticles may be able to modulate the distribution of drugs to other parts of the body.<sup>7-12</sup>

Azidothymidine (AZT) was chosen as a model antiviral drug since it represents the first and still one of the most important drugs in AIDS therapy.<sup>13</sup> It is usually given in com-

ination with other drugs to minimize drug resistance, toxicity, and side effects. Despite this approach, bone marrow toxicity, hematological changes, and short plasma half-life continue to limit the effectiveness of AZT therapy. Carrier systems for AZT such as nanoparticles offer in theory at least two advantages over current therapy. First, they can prolong the half-life of the drug in the body, reducing the dosing frequency and total dose required. Second, they can target AZT to the organs that are rich in macrophages. In earlier *in vitro* studies with human macrophage tissue cultures, it was shown that when AZT is bound to nanoparticles, it retains its full antiviral activity.<sup>3</sup> Moreover, chronically infected macrophages showed an even higher phagocytic activity than noninfected cells. This effect was even more pronounced with prolonged infections.<sup>14,15</sup>

In the present study the feasibility of the strategy to target drugs to the macrophages was tested using AZT as a model drug. In the first series of studies, free and nanoparticle-bound AZT was administered intravenously to rats, while in the second series, rats were given nanoparticles and control solutions orally.

Institut für Pharmazeutische Technologie, Johann Wolfgang Goethe-Universität, 60439 Frankfurt a.M., Germany.

\*Dedicated to Prof. Dr. K. Thoma, Ludwig-Maximilians-Universität, Munich, Germany, on the occasion of his 65th birthday.

## MATERIALS AND METHODS

### Synthesis of nanoparticles

Nanoparticles were produced by emulsion polymerization of 100  $\mu\text{l}$  of *n*-hexylcyanoacrylate monomer (Sichel Werke, Hannover, Germany) in 10 ml of an aqueous solution of 0.01 N HCl, containing 10 mg of [ $^{14}\text{C}$ ]AZT (Sigma, Deisenhofen, Germany) with an activity of 250  $\mu\text{Ci}$  as well as 20 mg of bis(2-ethylhexyl)sulfosuccinate sodium as an emulsifier (Fluka, Neu-Ulm, Germany). The monomer was added into the solution dropwise under mechanical stirring (600 rpm). After 96 hr the solution was neutralized with 100  $\mu\text{l}$  of a 1 N sodium hydroxide solution. Control solutions with the same [ $^{14}\text{C}$ ]AZT content were prepared identically, but without monomer.

### Determination of drug loading

An aliquot of 185  $\mu\text{l}$  of the suspension was centrifuged for 30 min at  $100,000 \times g$  using an Air Fuge (Beckman Inst., Munich, Germany). Unbound AZT was assayed by high-performance liquid chromatography (HPLC) of the supernatant. The HPLC analysis was performed using a Perkin-Elmer Series II pump with autosampling system ISS 100 and integrator LCI 100 (Perkin-Elmer, Langen, Germany). The analytical column (LiChroCART 125-4) was filled with LiChrospher 100 RP-18 (5  $\mu\text{m}$ ); the guard column was a LiChroCART 4-4 filled with the same material (Merck, Darmstadt, Germany). The mobile phase consisted of 15% acetonitrile–0.12 M phosphate buffer (pH 6.2)–14.4 mM triethylamine and the flow rate was 1.0 ml/min. All chemicals used for the HPLC assay were gradient grade. Ultraviolet (UV) detection was carried out at a wavelength of maximum absorbance, 265 nm, with a Lambda-Max 480 UV detector (Waters, Eschborn, Germany). About 48 to 55% of the AZT was adsorbed to the particles.

### Particle size

The particle size was measured by laser light scattering using a BI 200 SM goniometer with digital correlator linked to a PC (Brookhaven Instruments, Holtsville, NY). The average diameter of the particles was  $230 \pm 20$  nm, with a dispersity of  $>0.2$ .

### Animal experiments

The animals were kept under standard conditions, with free access to water and food. Nanoparticles and control solution were tested as an intravenous injection into the tail vein or were dosed perorally into the stomach by gavage. For each preparation and each sampling time point, four rats (two males and two females [Wistar Unilever rats, Harlan Winkelmann, Borchon, Germany], with a body weight of 180 to 220 g) were treated with a single dose of 3.33 mg of AZT (90.91  $\mu\text{Ci}$ )/kg body weight. After the administration of the preparation, the animals were kept in individual cages. Animals were sacrificed with  $\text{CO}_2$  after 5, 10, 15, 30 min, 1, 2, 4, and 8 hr (intravenous studies) and 0.5, 1, 2, 4, 6, and 8 hr (oral study). The animals were dissected and an aliquot was taken from each organ. Samples were accurately weighed into glass vials. After dissolving the tissue in 1 ml of BTS 450 tissue solubilizer (Beckman) at  $50^\circ\text{C}$ , 500  $\mu\text{l}$  of hydrogen peroxide solution (30%) was added until

the color was removed. After addition of 100  $\mu\text{l}$  of glacial acetic acid and 10 ml of liquid scintillation cocktail (Ready Organic; Beckman) samples were stored for 1 week in a light-free environment before radioactivity was determined in a scintillation counter (model LS 1801; Beckman).

### Autoradiography

The rat cadavers were placed into a gel containing 2% cellulose (Tylose C 600; Hoechst, Frankfurt, Germany) and were frozen in liquid nitrogen. Slices were cut using a microtome (Cryo Polycut; Leica, Benzheim, Germany). The slices were fixed onto an adhesive tape (Tesafilm, Beiersdorf, Hamburg, Germany) and freeze-dried in the microtome. Radioactivity was visualized by radioluminography using a bio-imaging analyzer (BAS 2000; Fuji Photo Film, Tokyo, Japan).

## RESULTS

Figure 1 shows the AZT concentration kinetics in the liver after intravenous injection. The liver concentrations of the [ $^{14}\text{C}$ ]AZT label were about 2.5- to 18-fold higher after binding to nanoparticles than after administration of the solution, with differences increasing with time. In other organs of the RES, the difference in the uptake rate was not as high as in the liver. Nevertheless, a significant difference between the two preparations occurred in these organs showing similar trends; in the lungs and in the spleen about 10-fold differences in favor of the nanoparticles were obtained after 480 min (Table 1). In bone marrow, the difference was about a factor of two after 480 min. In other organs, no relevant differences were observed. In some organs, administration resulted in lower AZT concentrations. After i.v. administration of nanoparticles, the total dose of AZT in the organs of the RES after 5 min amounted to 23%. The control solutions reached an uptake into the RES of only 9% by the same time. Four hundred and eighty minutes after nanoparticle injection, 60% of the detected AZT label was found in the RES, whereas only 12% of the label was found in the RES after in-

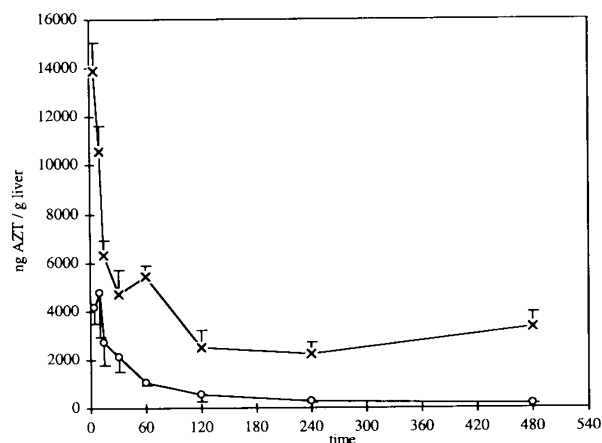


**FIG. 1.** [ $^{14}\text{C}$ ]AZT concentrations in the liver after i.v. injection of AZT (3.33 mg/kg) bound to nanoparticles ( $\times$ ) or in form of a solution, identically prepared but without monomer ( $\circ$ ). Every time point represents the average concentration of two male and two female rats of a body weight between 180 and 220 g.

TABLE 1. [<sup>14</sup>C] AZT CONCENTRATIONS IN BLOOD, BONE MARROW, BRAIN, LIVER, LUNGS, AND SPLEEN AFTER INTRAVENOUS INJECTION AND PERORAL ADMINISTRATION OF AZT BOUND TO NANOPARTICLES OR IN THE FORM OF A SOLUTION<sup>a</sup>

Organ	Time								
	5 min (mean ± SD)	10 min (mean ± SD)	15 min (mean ± SD)	30 min (mean ± SD)	60 min (mean ± SD)	120 min (mean ± SD)	240 min (mean ± SD)	480 min (mean ± SD)	
Blood									
<i>p</i> <sup>b</sup>				*	*		*		
nan	4158 ± 541	3092 ± 331	2854 ± 849	1772 ± 217	1040 ± 128	897 ± 179	577 ± 191	576 ± 366	
sol	3416 ± 329	3338 ± 480	2112 ± 186	1387 ± 273	894 ± 122	558 ± 87	342 ± 227	598 ± 124	
Bone marrow									
<i>p</i>								*	
nan	2177 ± 582	1951 ± 299	1754 ± 994	1751 ± 622	931 ± 317	762 ± 224	462 ± 132	319 ± 68	
sol	2631 ± 210	2433 ± 535	2795 ± 991	1864 ± 606	1098 ± 731	580 ± 303	312 ± 114	125 ± 47	
Brain									
<i>p</i>	*			*	*	*	*	*	*
nan	559 ± 72	514 ± 49	522 ± 236	331 ± 40	201 ± 17	118 ± 20	77 ± 7	58 ± 7	
sol	469 ± 48	489 ± 110	348 ± 49	420 ± 45	170 ± 20	93 ± 17	56 ± 6	61 ± 73	
Liver									
<i>p</i>	*	*	*	*	*	*	*	*	*
nan	13908 ± 1164	10569 ± 1061	6308 ± 619	4715 ± 999	5431 ± 414	2485 ± 725	2193 ± 505	3346 ± 608	
sol	4178 ± 705	4787 ± 1860	2707 ± 916	2107 ± 627	1074 ± 129	530 ± 264	287 ± 57	178 ± 27	
Lungs									
<i>p</i>	*	*	*	*	*	*	*	*	*
nan	6895 ± 1459	5477 ± 694	3388 ± 391	2063 ± 413	2778 ± 635	737 ± 161	839 ± 100	1464 ± 1111	
sol	4282 ± 485	3832 ± 928	2490 ± 367	1709 ± 245	671 ± 145	394 ± 171	169 ± 66	90 ± 10	
Spleen									
<i>p</i>	*	*	*	*	*	*	*	*	*
nan	5821 ± 785	3853 ± 637	3449 ± 556	2348 ± 199	3460 ± 1430	1648 ± 540	1281 ± 442	1489 ± 152	
sol	3260 ± 993	3059 ± 920	2569 ± 1612	2287 ± 954	665 ± 250	533 ± 348	279 ± 103	133 ± 18	

TABLE I. (Continued)

Organ	Time					
	30 min (mean $\pm$ SD)	60 min (mean $\pm$ SD)	120 min (mean $\pm$ SD)	240 min (mean $\pm$ SD)	360 min (mean $\pm$ SD)	480 min (mean $\pm$ SD)
Blood						
<i>p</i>			*			*
nan	366 $\pm$ 161	375 $\pm$ 65	265 $\pm$ 30	166 $\pm$ 66	224 $\pm$ 122	236 $\pm$ 62
sol	467 $\pm$ 215	361 $\pm$ 123	204 $\pm$ 39	161 $\pm$ 55	152 $\pm$ 28	122 $\pm$ 49
Bone marrow						
<i>p</i>			*			
nan	410 $\pm$ 234	522 $\pm$ 268	576 $\pm$ 30	293 $\pm$ 120	221 $\pm$ 57	145 $\pm$ 79
sol	722 $\pm$ 414	464 $\pm$ 189	368 $\pm$ 30	239 $\pm$ 93	194 $\pm$ 74	164 $\pm$ 64
Brain						
<i>p</i>			*	*	*	*
nan	118 $\pm$ 75	133 $\pm$ 35	77 $\pm$ 39	80 $\pm$ 13	72 $\pm$ 12	59 $\pm$ 4
sol	116 $\pm$ 61	100 $\pm$ 28	57 $\pm$ 25	62 $\pm$ 10	44 $\pm$ 5	44 $\pm$ 6
Liver						
<i>p</i>			*		*	*
nan	872 $\pm$ 449	921 $\pm$ 250	784 $\pm$ 135	573 $\pm$ 88	448 $\pm$ 72	320 $\pm$ 68
sol	1418 $\pm$ 614	1113 $\pm$ 556	437 $\pm$ 92	375 $\pm$ 108	234 $\pm$ 52	214 $\pm$ 65
Lungs						
<i>p</i>			*		*	*
nan	461 $\pm$ 187	526 $\pm$ 89	312 $\pm$ 41	170 $\pm$ 31	136 $\pm$ 14	103 $\pm$ 13
sol	738 $\pm$ 424	552 $\pm$ 196	218 $\pm$ 50	156 $\pm$ 61	90 $\pm$ 16	80 $\pm$ 18
Spleen						
<i>p</i>	*				*	*
nan	413 $\pm$ 158	873 $\pm$ 563	397 $\pm$ 77	267 $\pm$ 85	184 $\pm$ 43	152 $\pm$ 27
sol	982 $\pm$ 373	771 $\pm$ 517	365 $\pm$ 177	212 $\pm$ 73	130 $\pm$ 17	100 $\pm$ 27

<sup>a</sup>Identically prepared but without monomer.

<sup>b</sup>\*, Statistically significant difference ( $p < 0.05$ ).

Abbreviations: SD, standard deviation; nan, nanoparticle preparation; sol, solution.

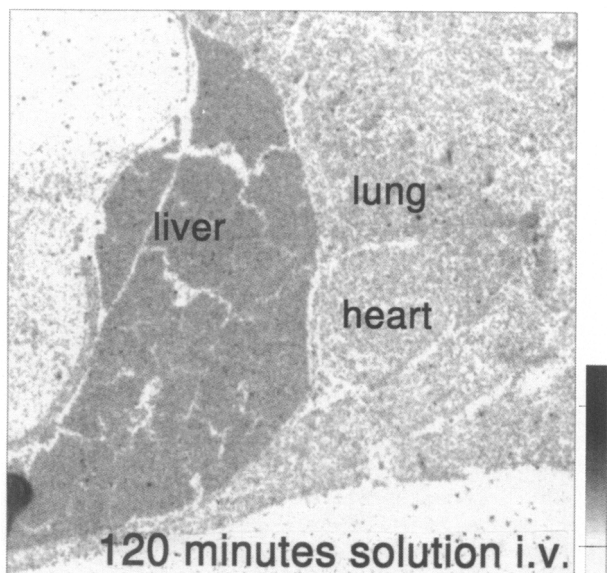


**FIG. 2.** Autoradiographic image of a rat 120 min after i.v. injection of [ $^{14}\text{C}$ ]AZT (3.33 mg/kg) in the form of a solution. AZT was homogeneously distributed in the liver tissue and the lung. Up to 94% of the AZT was eliminated via kidneys.

jection of the control solution. AZT bound to nanoparticles was eliminated to an extent of  $28\% \pm 5.8$  in the feces. AZT given in solution form was eliminated via the kidneys to an extent of  $94\% \pm 0.7$ . Autoradiographs after i.v. injection of the solution (Fig. 2) showed a rather homogeneous although sparse distribu-

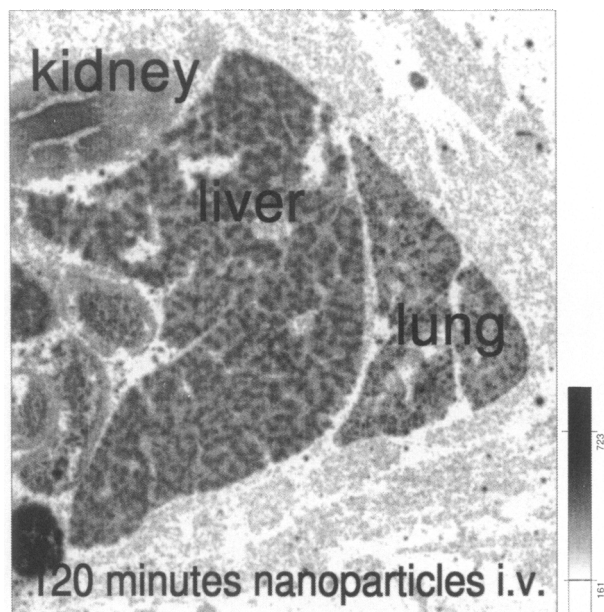


**FIG. 3.** Autoradiographic image of a rat 120 min after i.v. injection of [ $^{14}\text{C}$ ]AZT (3.33 mg/kg) bound to nanoparticles. AZT was inhomogeneously distributed in the liver tissue and the lung. Up to 28% of the AZT nanoparticle preparation was eliminated by feces.

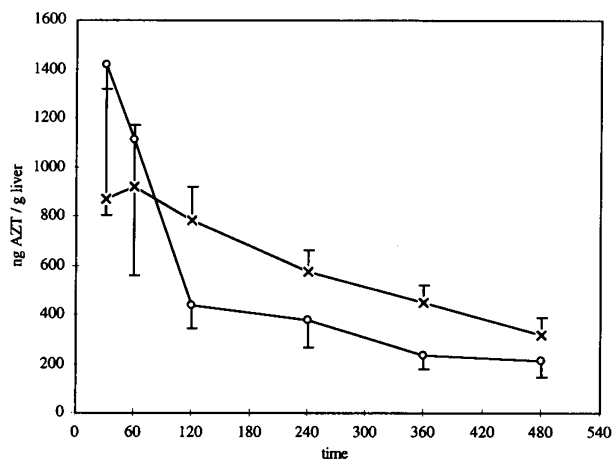


**FIG. 4.** [ $^{14}\text{C}$ ]AZT concentrations in the liver after peroral administration of AZT (3.33 mg/kg) bound to nanoparticles (X) or in the form of a solution, identically prepared but without monomer (O). Every time point represents the average concentration of two male and two female rats of a body weight between 180 and 220 g.

tion of the AZT label in liver and lungs, whereas after i.v. administration of nanoparticles (Fig. 3) the radioactive concentrations were much higher. In this case, not only was the concentration higher, but it appeared in clusters. These clusters were ascribed to macrophages (J. Maas, autoradiography specialist, Hoechst AG). In an earlier work (Waser *et al.*<sup>16</sup>) a similar appearance of radioactivity in the form of dots was identified as an accumulation of nanoparticles in macrophages by the combination of macro- and microautoradiography.

In the oral study (Fig. 4), similar results were found. Nanoparticles again led to an accumulation of AZT in tissues containing a large number of macrophages (Table 1). In the brain, the uptake of AZT was also higher when using nanoparticles as the drug-targeting system. This higher uptake was especially significant ( $p < 0.05$  after 2 hr) after oral administration. However, oral absorption of AZT from the solution was very rapid whereas binding of drug to nanoparticles delayed oral absorption. After administration of nanoparticles, 60 min was required to reach the highest concentrations in the RES organs. After oral administration, the bioavailability was 28% (nanoparticle preparation) and 30% (solution), respectively, compared to the i.v. injection.

During the first 2 hr after oral administration, the AZT concentration following administration of the control solution decreased by a factor of two to five, depending on the organ. At later times the organ clearance rate was considerably reduced, depending on the organ. Nanoparticles delivered AZT more slowly to all organs, and also resulted in a slower elimination. As a consequence 1.79% of the administered dose was still found after 480 min in contrast to 1.16% of the control. Both effects result in a better bioavailability of AZT bound to nanoparticles, particularly in the RES.

## DISCUSSION

Apart from the CD4 helper T subset of lymphocytes, cells of the mononuclear phagocyte system can be infected by

HIV-1 and HIV-2 strains.<sup>2,17,18</sup> For MO/MAC the virus seems to be much less cytotoxic than for T cells. Therefore, cells of the MO/MAC lineage most likely play an important role in the immunopathogenesis of the HIV infection, by serving as a reservoir for the virus and its dissemination throughout the body and brain.<sup>4,5</sup>

In the present study the AZT was chosen as a classic model compound for the treatment of AIDS. The finding by Schäfer *et al.*<sup>14</sup> that infected macrophages take up nanoparticles to a significantly higher degree than uninfected macrophages, and that this effect increases after longer time periods, may enable the use of drugs such as AZT even against chronically infected cells. The binding of AZT to nanoparticles does not decrease its antiviral activity against HIV.<sup>3</sup> In another *in vitro* study with acutely and chronically infected MO/MAC, the antiviral activity of saquinavir was highly increased when the drug was bound to nanoparticles compared to the solution.<sup>19</sup> The binding of AZT to the nanoparticles was stable for at least 2 weeks.

The results of the present study show that AZT bound to nanoparticles caused a higher drug uptake into the RES. Responsible for this uptake are macrophages, as confirmed by autoradiography (Fig. 3). The autoradiograms show that AZT bound to nanoparticles accumulated preferentially in the Kupffer cells of the liver. Our results are in agreement with earlier body distribution studies using nanoparticles conducted by Tröster *et al.*<sup>10</sup> and Illum *et al.*<sup>20</sup> In these earlier studies, the particle polymers were radiolabeled whereas in the present study the label was carried by the drug, AZT, itself. The conclusion that can be drawn from all of these studies is that nanoparticles can indeed be used for the targeted delivery of drugs such as AZT to the RES. The elimination pathway as well as the organ distribution are influenced by nanoparticles. Nefzger *et al.* demonstrated that nanoparticles were excreted to a large extent via the bile.<sup>21</sup> Similar results have been detected in our studies.

Furthermore, earlier results by Maincent *et al.*,<sup>22</sup> Dange *et al.*,<sup>23</sup> and Beck *et al.*<sup>24</sup> had shown that nanoparticles loaded with different drugs can increase oral bioavailability. Especially noteworthy for AIDS therapy is the finding that the brain concentration of AZT label after 1 hr was  $27 \pm 9\%$  higher after oral administration of nanoparticles compared to the control solution. Consequently, nanoparticles represent a very promising drug targeting system for AZT and perhaps also for AIDS therapy in general.

## ACKNOWLEDGMENTS

The authors thank the German Health Administration and the Frankfurter AIDS Project for their support of this project, and Dr. J. Maas (Hoechst AG, HMR Preclinical Development Pharmacokinetics Germany) for his help in processing the autoradiograms.

## REFERENCES

- Gendelman HE, *et al.*: The macrophage in the persistence and pathogenesis of HIV infection. *AIDS* 1989;3(8):475-495.
- Von Briesen H, *et al.*: Infection of monocytes/macrophages by HIV *in vitro*. *Res Virol* 1990;141:225-231.
- Bender A, *et al.*: Inhibition of HIV *in vitro* by antiviral drug-targeting using nanoparticles. *Res Virol* 1994;145(3-4):215-220.
- Roy S and Wainberg MA: Role of the mononuclear phagocyte system in the development of acquired immunodeficiency syndrome (AIDS). *J Leuk Biol* 1989;43:91-97.
- Meltzer MS, *et al.*: Macrophages and the human immunodeficiency virus. *Immunol Today* 1990;11(6):217-223.
- Kreuter J: Nanoparticles. In: *Colloidal Drug Delivery Systems*. (Kreuter J, Ed.). Marcel Dekker, New York, 1994, pp. 219-342.
- Kreuter J: Evaluation of nanoparticles as drug-delivery systems. II. Comparison of body distribution of nanoparticles with the body distribution of microspheres (diameter >1  $\mu\text{m}$ ), liposomes, and emulsions. *Pharm Acta Helv* 1983;58(8):217-226.
- Kreuter J: Factors influencing the body distribution of polyacrylic nanoparticles. In: *Drug Targeting* (Buri P and Gumma A, Eds.). Elsevier Science Publishers BV, Amsterdam, 1985, pp. 51-63.
- Illum L, Davis SS, Müller RH, Mak E, and West P: The organ distribution and circulation time of intravenously injected colloidal carriers sterically stabilized with a block polymer—poloxamine 908. *Life Sci* 1987;40:367-374.
- Tröster SD, Müller U, and Kreuter J: Modification of body distribution of poly(methyl-methacrylate) nanoparticles in rats by coating with surfactants. *Int J Pharm* 1990;61:61-85.
- Borchard G, Audus KL, Shi F, and Kreuter J: Uptake of surfactant-coated poly(methyl methacrylate)-nanoparticles by bovine brain microvessel endothelial cell monolayers. *Int J Pharm* 1994;110:29-35.
- Adachi N, Maruyama A, Ishihara T, and Akaike T: Cellular distribution of polymer particles bearing various densities of carbohydrate ligands. *J Biomaterials Sci* 1994;6(5):463-479. [Polymer edition]
- McLeod G and Hammer S: Zidovudine: Five years later. *Ann Intern Med* 1992;117:487-501.
- Schäfer V, *et al.*: Phagocytosis of nanoparticles by human immunodeficiency virus (HIV)-infected macrophages: A possibility for antiviral drug targeting. *Pharm Res* 1992;9(4):541-546.
- Schäfer V, Kreuter J, Rübbsamen-Waigmann H, Gerte S, and Von Briesen H: Influence of HIV-infection on the phagocytic activity of monocytes/macrophages and granulocytes. *Clin Diagn Virol* 1994;1:279-287.
- Waser PG, *et al.*: Localization of colloidal particles (liposomes, hexylcyanoacrylate nanoparticles and albumin nanoparticles) by histology and autoradiography in mice. *Int J Pharm* 1987;39:213-227.
- Kühnel H, *et al.*: Molecular cloning of two West African human deficiency virus type 2 isolates that replicate well in macrophages: A Gambian isolate, from a patient with neurologic acquired immunodeficiency syndrome and a highly divergent Ghanian isolate. *Proc Natl Acad Sci USA* 1989;86:2383-2387.
- Gendelman HE, *et al.*: Efficient isolation and propagation of human immunodeficiency virus on recombinant colony-stimulating-factor-1-treated monocytes. *J Exp Med* 1988;167:1428-1441.
- Bender A, Von Briesen H, Kreuter J, Ducan IB, and Rübbsamen-Waigmann H: Efficiency of nanoparticles as carrier system for antiviral agents in human immunodeficiency virus-infected human monocytes/macrophages *in vitro*. *Antimicrob Agents Chemother* 1996;40(6):1467-1471.
- Illum L, Davis SS, Wilson CG, Thomas NW, and Hardy JG: Blood clearance and organ deposition of intravenously administered colloidal particles. The effects of particle size, nature, and shape. *Int J Pharmacol* 1982;12:135-146.
- Nefzger M, Kreuter J, Voges R, Liehl E, and Czok R: Distribution and elimination of polymethyl-methacrylate nanoparticles after peroral administration to rat. *J Pharm Sci* 1984;73(9):1309-1311.
- Maincent P, Verge RL, Sado P, Couvreur P, and Devissaguet JP: Disposition kinetics and oral bioavailability of vincamine loaded

- polyalkylcyanoacrylate nanoparticles. *J Pharmacol Sci* 1986;75: 955–958.
23. Damge C, *et al.*: Polyalkylcyanoacrylate nanocapsules increase the intestinal absorption of a lipophilic drug. *Int J Pharm* 1987;36: 121–125.
24. Beck PH, Kreuter J, Müller WEG, and Schatton W: Improved peroral delivery of avarol with polybutylcyanoacrylate nanoparticles. *Eur J Biopharm* 1994;40(3):134–137.

Address reprint requests to:

*Jörg Kreuter*  
*Institut für Pharmazeutische Technologie*  
*Johann Wolfgang Goethe-Universität*  
*Marie-Curie Straße 9*  
*60439 Frankfurt a.M., Germany*